

Original Article

HOG and Haralick Feature Extractions with Machine Learning Methods for Covid-19 X-Ray Image Classification

Nurul Nadiah Abd Rahman¹, Marina Yusoff^{1,2}, Murizah Kassim³

¹Faculty of Computer and Mathematical Science, Universiti Teknologi MARA, Shah Alam, Malaysia

²Institute for Big Data Analytics and Artificial Intelligence (IBDAAI), Universiti Teknologi MARA, Shah Alam, Malaysia

³School of Electrical Engineering, College of Engineering, Universiti Teknologi MARA, Shah Alam, Malaysia

²Corresponding Author : marina998@uitm.edu.my

Received: 05 July 2022

Revised: 25 September 2022

Accepted: 05 October 2022

Published: 19 October 2022

Abstract - Distinguish COVID-19 from other respiratory diseases remains a demand mainly in machine learning solutions. The overlapping symptoms can confuse identifying the type of disease and lead to misdiagnosis. This paper evaluates feature extraction methods in conjunction with machine learning to determine a positive COVID-19 class. Pre-processing operations on a benchmark COVID-19 x-ray images dataset include under-sampling, resizing, converting into grayscale images, and noise removal. These operations are carried out to reduce the data produced by the dataset. A hybrid approach was used to conduct the evaluation, with Histogram of Oriented Gradient and Haralick as feature extractor methods and Support Vector Machine and K-Nearest Neighbors as classifiers. Several different parameters help measure the classifiers' performance. Compared to other hybrid methods, the Support Vector Machine with a Histogram of Oriented Gradient feature extraction performed the best. It has the highest accuracy score possible, coming in at 93.31%. The feature extraction method contributes to higher performance in the x-ray image classifier. In the future, additional feature extraction strategies, such as deep learning, may be potential competitors to this work.

Keywords - COVID-19, Feature Extraction, Machine Learning, Support Vector Machine, K-Nearest Neighbors.

1. Introduction

SARS-CoV-2 is a subset of the Coronaviruses (CoVs) group. CoVs group consists of highly diverse, enveloped, positive-sense, and single-stranded RNA viruses [1]. This virus might have been transmitted to humans by pangolins or other animal hosts. However, the virus's global spread is caused by respiratory droplets through physical contact with human-to-human transmission [2]. The common symptoms of COVID-19 are dry cough, fever, dyspnea, diarrhea, headache, shortness of breath, and bilateral lung infiltrates [3]. They state that late detection of COVID-19 might cause patients to develop severe COVID-19 and critical complications, such as cardiac injury and acute respiratory distress syndrome. Hence, early detection of COVID-19 is needed to prevent the spread of the virus and prevent patients from developing severe COVID-19 illnesses.

One way to diagnose or detect COVID-19 patients is by using chest x-ray (CXR) images. CXR images significantly differ in the chest images of positive and negative COVID-19 patients. According to [4], usually, positive COVID-19 patients show the presence of bilateral radiographic abnormalities in CXR images. Chest images can help detect

COVID-19 by using specific techniques, such as machine learning algorithms, deep learning algorithms, convolutional neural networks, and transfer learning [5-8]. However, different methods produce different accuracy, sensitivity, and specificity rates.

Furthermore, it is hard to distinguish COVID-19 from other respiratory diseases because they share similar symptoms [9]. For example, fever, dry cough, shortness of breath, and sore throat are the common symptoms of both COVID-19 and the flu. Besides, COVID-19, pneumonia, and acute respiratory distress syndrome have the same gastrointestinal symptoms, such as diarrhea, vomiting, nausea, and anorexia [34]. It will contribute to late COVID-19 detection and rapid spread of COVID-19, as they do not seek medical care and have poor awareness of COVID-19 prevention [11].

Much work on the classification of the images from various domains [12-14]. CXR images, mainly for COVID-19 CXR images are still in research demand. Research on COVID-19 CXR images using the most recent deep



convolutional neural networks [12]. In this work, class decomposition steps involve using different pre-trained CNN models like VGG19 to extract features and create a deep feature space from the images. Principle Component Analysis (PCA) is also used to reduce the dimension of deep feature space. The proposed solution achieved a high accuracy of 93.1% by using the VGG19 pre-trained CNN model.

Furthermore, a finding by [14] has developed a predictive model for COVID-19 based on CXR images to identify the available learning image categories at a fast pace using a small sample size. The proposed model used the concept of one-shot cluster-based learning. One-cluster based-learning is a process of human learning using a few examples. Generalized Regression Neural Networks and Probabilistic Neural Networks were used to classify the images into four classes: pneumonia bacterial, pneumonia virus, and normal COVID-19. A total of 306 chest x-ray images are collected from the publicly available dataset by Joseph Cohen. Based on the results obtained, the proposed model can differentiate chest x-ray images in the COVID-19 class more effectively compared to the other three categories since the COVID-19 class achieved an accuracy of 85.23%, while 63.29% accuracy for pneumonia bacterial, 61.84% accuracy for pneumonia virus and 65.80% accuracy for normal class. The model also performs better than other deep learning models like AlexNet, GoogleNet, and ResNet as it has less training time and simple calculations. Based on the previous research that has been conducted, both CNN and machine learning can produce high accuracy and have better performance in image classification. However, the machine learning method could be more suitable for dealing with smaller datasets than the CNN method.

CNN can perform feature extraction. As for a small dataset of less than 10000. Other feature extraction methods to comply with machine learning methods, such as SVM and KNN, should be evaluated further. One of the potential feature extractors is the Histogram of Oriented Gradients (HOG), as it is known to be more energy-efficient than CNN [15]. It is also evident that deep learning algorithms consume much time during training [16]. HOG involves a feature extractors strategy and uses a simple computation. It has a good capability in extracting features from image data. It works by the edge direction and is based on a gradient to decompose into smaller regions [17].

Another potential feature extraction is Haralick, an image texture analysis that utilizes spatial gray tone co-occurrence texture features. It is suitable for image extraction, where a region of interest determination is on a square matrix of the dimension gray value [18]. Haralick texture is one of the fast calculation formulations in feature extraction [19]. These features are calculated from the Gray Level Co-occurrence Matrix (GLCM), a matrix that counts

the co-occurrence of nearby gray levels in the image. To calculate the GLCM and Haralick features. This method utilizes the joint probability distributions of pixel pairs. As a function of the grey level, GLCM displays the frequency with which each grey level at a pixel on a fixed geometric relative position to each other pixel. Haralick method has high potential in improving feature extraction ability as it is still widely used, especially in image feature determination [20]. Harlick was used in many image detection domains [21-22]. Therefore, this paper aims to evaluate HOG and Haralick feature extraction methods using machine learning to detect a positive COVID-19 class using CXR images.

2. Related Work

Numerous studies and findings have been conducted and applied to detect COVID-19 using chest x-ray images. These studies employ various techniques and procedures, including machine learning algorithms, convolutional neural networks transfer learning, and deep learning algorithms. Some reviewed research utilized the same domain with similar or distinct techniques, while others used different domains with the same methods. It proposed a rapid and automatic COVID-19 detection system utilizing chest x-ray images [23]. In image processing, the robust features algorithm and K-means clustering extract and cluster feature descriptors from images. In the meantime, SVM classifiers, one of the machine learning classifiers, assist in identifying the appearance of COVID-19 viruses in the images. SVM classifiers are also accountable for classifying images as positive for COVID-19 or healthy. They used two distinct types of datasets, distinct from the dataset for this study. These two datasets include 170 chest radiograph images for both COVID-19-positive and healthy subjects. The SVM classifier proposed method is compared to the CNN model. According to the findings, SVM classifiers produced superior results and achieved a higher accuracy rate of 94.12% than CNN classifiers. This is due to CNN's effectiveness with larger datasets. SVM classifier has the limitation of requiring a longer running time than CNN. Despite this, both the SVM classifier and CNN can make precise and timely COVID-19 predictions.

Researched to classify COVID-19 chest x-ray images using deep convolutional neural networks. Decompose, Transfer, and Compose is another name for this deep convolutional neural network (DeTraC) [24]. For normal and positive COVID-19 classes, 80 and 116 chest x-ray images are used. COVID-19 detection from chest x-ray images involves class decomposition, transfer learning, and class composition. Class decomposition involves various pre-trained CNN models, such as VGG19, to extract image features and generate a deep feature space.

PCA is also used to reduce the dimension of deep feature space throughout that step. Next, the objective of transfer learning is to test, compare, and evaluate various

pre-trained CNN models. The composition phase, the execution, will aid in improving the classification of the images. The proposed DeTraC achieved a high level of accuracy of 93.1% by employing a pre-trained VGG19 CNN model and a sensitivity rate of 100%. A predictive model for COVID-19 using chest x-ray images [14] is to rapidly identify the available learning image categories using a small sample size. The proposed model used the concept of cluster-based learning in a single instance. One-cluster based-learning is a human learning method that employs a few examples. The proposed model can differentiate chest x-ray images in the COVID-19 class more effectively than in the other three classes, as the COVID-19 class achieved an accuracy of 85.23 percent, compared to 63.29% for pneumonia bacterial, 61.84% for pneumonia virus, and 65.80 percent for the normal class. The model outperforms other deep learning models such as AlexNet, GoogleNet, and ResNet due to its shorter training time and straightforward calculation.

In addition, referencing a study by [7], an automated prediction model for COVID-19 was proposed. Chest x-rays are used to determine whether a patient has contracted this disease. Using CNN and transfer learning algorithms, these images will be classified into three classes: positive COVID-19, other pneumonia infection, and no infection. VGG-16 and ResNet-50 are the two methods used in transfer learning algorithms. In total, 2,905 chest images were collected by Rahman et al. and included in this study's dataset (2021). Two hundred nineteen chest x-ray images correspond to the positive COVID-19 class, 1,345 images correspond to other pneumonia infection classes, and 1,341 images do not conform to any infection class. According to the proposed method's results, the VGG-16 model has a higher accuracy of 97.67% than CNN and ResNet-50, which generate an accuracy of 93.67% and 96.47%, respectively. Machine learning algorithms can identify and forecast COVID-19 and classify chest x-ray images. Predictive models for COVID-19 diagnosis have been developed using fourteen clinical features, including the white blood cell count (WBC), Eosinophil (E%), Neutrophil (N%), Lymphocyte (L%), Neutrophil-Lymphocyte (N/L), Monocytes (M%), Lymphocyte-Monocyte (L/M), Basophils (B%), Hemoglobin (Hb), Hematocrit (Pro) [25]. This study employed six distinct classifiers, including the Bayes classifier (BayesNet), the logistic-regression classifier (Logistic), the lazy-classifier (Blk), the CR meta-classifier, the rule-learner (PART), and the decision tree classifier (J48). It is only concerned with Chinese COVID-19 patients. Taizhou Hospital in Zhejiang Province collected the clinical characteristics of 114 COVID-19 patients between 17 January 2020 and 17 February 2020. With an accuracy of 84.12%, the CR meta-classifier is the most accurate classifier for predicting COVID-19 based on the results obtained. The performance of CR meta-classifiers is also superior to that of the other five classifiers. Despite

this, this study does not consider the COVID-19 symptoms in diagnosing the disease due to the paucity of data.

COVID-19 can be predicted using epidemiology data [26]. The General Directorate of Epidemiology of the Mexican Secretariat of Health compiled the epidemiology dataset. COVID-19 patients in Mexico are represented by 263,007 data and 41 attributes, including demographic data, clinical data, and RT-PCR test results. There are two collected demographic variables: gender and age. In the meantime, clinical data, including pneumonia, obesity, asthma, diabetes, cardiovascular diseases, chronic kidney diseases, hypertension, and tobacco, have been recorded. Since it employs supervised machine learning algorithms, this dataset also includes the targeted class output, denoted by 1 for positive and 0 for negative classes. The dataset is divided into a training set of 80% and a testing set of 20%. The prediction model is developed using Nave Bayes, logistic regression, decision tree, support vector machine, and ANN. Using the decision tree model, the proposed model achieves high accuracy of 94.99%, while the SVM model achieves the highest sensitivity rate of 93.34%. Using the Nave Bayes model, it is possible to achieve a specificity rate of 94.30 percent.

Machine learning algorithms detect diseases such as pneumonia and malaria. Machine learning classifiers can aid in predicting pneumonia [27]. For the classification process, 5,856 chest x-ray images comprised 1,583 normal chest images and 4,273 positive Pneumonia infection images. This dataset is divided into 80% training set data, 10% testing set data, and 10% validation set data. The prediction model is constructed using CNN, Random Forest, KNN, AdaBoost, Gradient Boost, XGBoost, and deep learning algorithms. Fivefold and tenfold cross-validation is used to evaluate each technique. The accuracy of the proposed CNN model is 98.42%, which is higher than the accuracy of the other six techniques. For the testing set, Random Forest achieves a high level of accuracy of 97.61%. A separate study proposed a Malaria prediction model based on algorithms for machine learning. In this study, SVM and ANN are the machine learning classifiers employed in 1,680 malaria-related data [35]. According to the results, SVM models are more accurate and generate a lower error rate than ANN models.

3. Materials and Methods

3.1. System Architecture

Figure 1 depicts the main steps of the proposed method system architecture. The procedures involve adding images, processing them beforehand, extracting features, dividing images, classifying them, and evaluating the results. The patient's chest x-ray images are entered first to begin the process. Then, all images will undergo under-sampling to overcome imbalanced class problems. Then, the chest x-ray images will be resized as some images have different sizes.

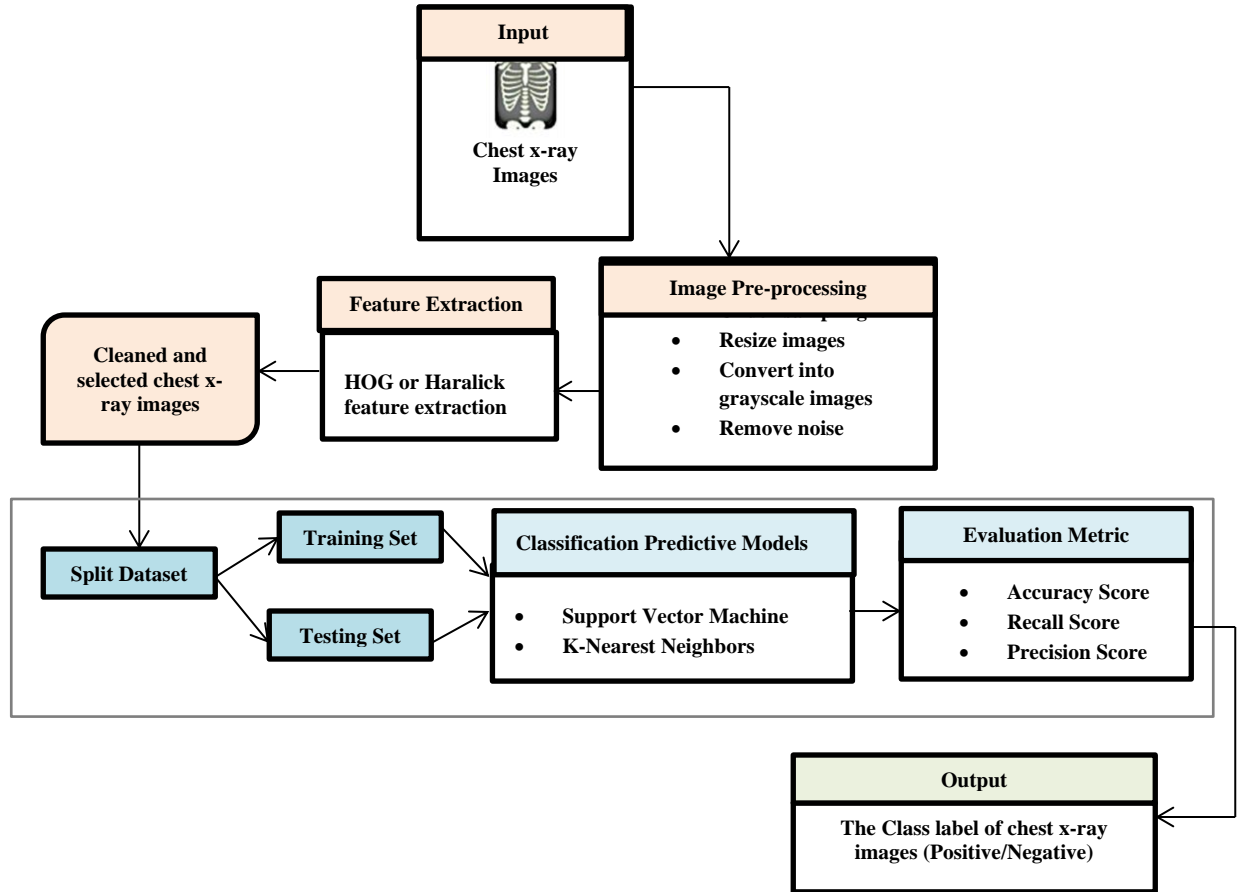


Fig. 1 System Architecture

After that, all the images will be converted into grayscale images. Noise on the images will also be removed to maintain the quality of the data. The next step is the feature selection process. Feature selection reduces the number of input variables to reduce the computational cost and improve the machine learning algorithm's performance. The cleaned and selected dataset will subsequently be divided into two sets, training and testing. Then, the images will be fed into the classification model to detect the probability of data in the positive and negative classes. SVM and KNN are the two machine learning classifiers used in this research. This model will train, test, and evaluate the performance of the models using a testing set. The evaluation metrics will compare and select the most suitable classification predictive model, including accuracy, specificity, and sensitivity scores.

3.2. Datasets

A CXR images datasets used in this study is one of the popular public X-ray data. The CXR images consisted of 3,616 chest x-ray images for the COVID-19 class and 10,192 for the normal class [29]. However, the evaluation considered balanced data from 3,616 chest x-ray images for positive COVID-19 and negative COVID-19 classes.

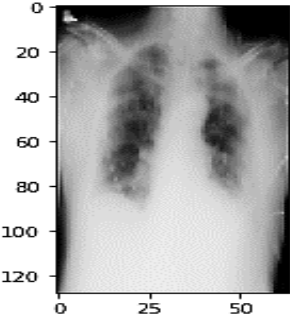
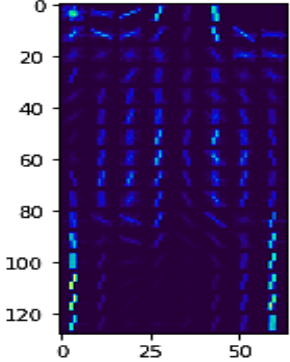
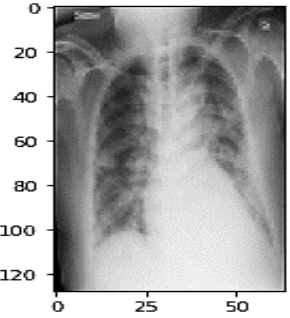
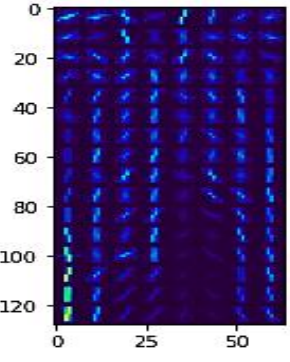
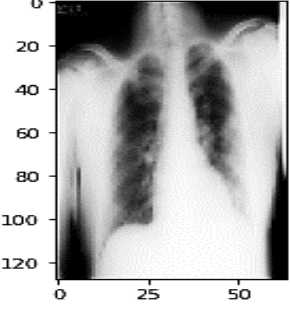
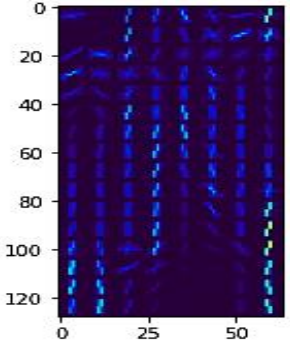
3.3. Pre-processing

All chest x-ray images were resized and rescaled from 299 x 299 pixels to 64 x 128 pixels since the images were collected from four countries. Each country used different types of devices that produced various images. Next, convert the RGB chest x-ray images into grayscale images. After conducting this process, the result was that less information was stored for each pixel, reducing the model's training time. After that, impulse or salt-and-pepper noise on the grayscale images was removed using the median blur function.

3.4. Feature Extraction

Feature extraction was conducted using two methods: HOG and Haralick feature extractions. HOG is one of the feature descriptors for image detection. The HOG descriptor focuses on the structure or the shape of an object. It is better than any edge descriptor because it uses the gradient's magnitude and angle to compute the features. The image regions generate histograms utilizing the volume and orientations of the gradient. HOG features have been extracted for each pre-processed image of dimension (64 × 128) as suggested in a few works of literature [16].

Table 1. Example of Results of feature extraction using HOG

Smooth Images	Result of Feature Extraction using HOG
	
	
	

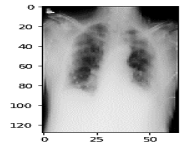
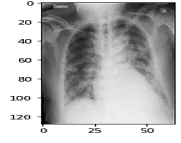
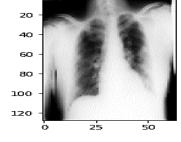
Haralick texture feature extraction is based on Gray Level Co-occurrence Matrix calculation. It is a matrix that counts the co-occurrence of nearby gray levels in images. It resulted in a new reduced set of features being created, containing summarized information from the original set. Tables 1 and 2 show the six samples of the smooth images and the result after extracting features using HOG and Harallick feature extractors. HOG feature extraction produces results in images, while Harallick results are in arrays as it calculates the average values of the features.

3.5. Support Vector Machine

Support vector machine or also known as SVM classifier. This classification algorithm was found by Boser,

Guyon, Cortes, and Vapnik. SVM classifier is called Maximum Margin classifier since it has a unique characteristic that can reduce the observed classification error and enlarge the geometric margin concurrently [30-31]. In SVM classification, data points in space are separated by a dividing plane or hyperplane [30]. The hyperplane is located where class labels are placed on each side of the hyperplane [31], and the maximum distance from every side to the nearest vector is the optimum margin. SVM classification algorithm can produce better performance in accuracy rate than other classification algorithms.

Table 2. Results of feature extraction using Haralick

Smooth Images	Result of Feature Extraction Using Haralick
	[2.13881515e-03 1.15335955e+02 9.77342904e-01 2.56094150e+03 3.65577361e-01 2.93767148e+02 1.01284300e+04 8.10380823e+00 1.07240916e+01 5.73160812e-04 3.75593172e+00 -4.98049078e-01 9.99442750e-01]
	[6.87563155e-04 5.89058926e+01 9.81216534e-01 1.57371961e+03 3.08871776e-01 2.83491939e+02 6.23597254e+03 8.16268803e+00 1.12054685e+01 4.62219588e-04 3.74975152e+00 -4.40943447e-01 9.98843822e-01]
	[2.39875750e-03 2.52105061e+02 9.76102083e-01 5.28340940e+03 2.94458530e-01 3.06509722e+02 2.08815325e+04 8.54959130e+00 1.15527869e+01 3.29401987e-04 4.41182294e+00 -4.77864744e-01 9.99508342e-01]

3.6. K-Nearest Neighbors

K-Nearest Neighbors or KNN classification algorithm. KNN classifiers group similar objects nearest to each other in the feature space. Also, this classifier is the most straightforward classification algorithm since the classification process only considers the labels of objects closest to them by a majority vote. Furthermore, KNN classifiers are lazy learners because it only involves two steps: storing all information on training samples and creating a classifier if a new and unlabeled test sample needs to be classified [32]. Two methods to assign class labels for an object is acquiring a majority vote of the K nearest reference points [29]. The advantages of KNN classifiers include simple implementation, ease of understanding, fast training time, and robustness towards noisy training data [33]. Despite that, KNN classification algorithms can cause classification errors if only a few features are available for the classification process [32].

4. Computational Result and Discussion

4.1. Parameter Settings

As for SVM, three models were experimented with to fine-tune the kernel, C, and gamma parameter values to find the best combination of hyperparameters and high accuracy scores. Kernel functions are a collection of mathematical functions that assist in transforming input data into the required form of processing data. The kernels are linear, polynomial, and radial basis functions (RBF). For KNN, three experiments involving these models of fine-tuning the k parameter value to find the best combination of hyperparameters and high accuracy scores. The K parameter refers to the number of closest neighbors that should be included in the majority of the voting procedure. KNN models were trained with different split ratios, 50:50, 60:40, 70:30, 80:20, and 90:20, for each experiment. Every experiment used various KNN models for the training process, including the basic KNN model, KNN with HOG

feature extraction, and KNN with Haralick feature extractor. Each KNN model also was trained with different k values. In the first experiment, the k value was set to 85. The optimal k value equals the square root of the total number of samples. K value was set to 45 and 5 for the other two experimental works.

4.2. Computational Result using Variants of SVM Models

For the first experiment, the kernel function of the SVM models was set to a linear kernel. Linear kernels are one of the most common kernels used by other researchers. This kernel is usually used when the data is linearly separable, which means it can be separated using a single line. This kernel consists of two main parameters, gamma and C. Table 3 shows the accuracy, precision, and recall scores obtained in the first experiment for all three SVM models; based on the training and testing split percentage. The three classification models achieved an accuracy score. The accuracy value represents the number of chest x-ray images that the classification models could correctly classify into COVID-19 and normal classes. When using a 90:10 training testing split ratio, all three types of SVM models achieved the highest accuracy values. The maximum accuracy of SVM, SVM with HOG feature extraction, and SVM with Haralick feature extractor was 83.56%, 88.12%, and 74.17%, respectively.

Moreover, during the 50:50 training testing split ratio, the SVM model had the lowest accuracy of 79.97%. The SVM with HOG feature extraction and the Haralick feature extractor had the most insufficient accuracy of 86.27% and 71.31%, respectively, during the 60:40 training testing split ratio. Overall, the SVM with HOG feature extraction performed better and produced an excellent accuracy value compared to the other two models. SVM with the Haralick feature extractor had the worst performance and scored the lowest accuracy among the three trained and tested models. Overall, SVM with HOG feature extraction had the most outstanding recall value among the three models. In

contrast, SVM with the Haralick feature extraction model had the least recall value of the other two classification models. The SVM with HOG produced the highest precision of the other two models, whereas the SVM with the Haralick feature extractor model had the lowest precision score.

As shown in Table 3, the accuracy score was achieved by the three classification models based on Polynomial Kernel. The SVM model achieved the highest accuracy value of 91.02% during the 90:10 training testing split ratio. Meanwhile, both SVM with HOG feature extraction and SVM with Haralick feature extractor had the maximum accuracy value of 93.31% and 50.50%, respectively, during the 70:30 training testing split percentage. Moreover, during the 50:50 training testing split ratio, the SVM and SVM with HOG feature extraction models had the lowest accuracy of 89.07% and 91.92%, respectively. In comparison, the SVM with the Haralick feature extractor had the most insufficient accuracy of 47.68% during the 80:20 training testing split ratio. Overall, the SVM with HOG feature extraction performed better and produced the most remarkable accuracy value compared to the other two models.

In contrast, SVM with the Haralick feature extractor had the worst performance and made the lowest accuracy score among the three trained and tested models. SVM with HOG feature extraction had the most outstanding recall value among the three models. In contrast, SVM with the Haralick feature extraction model had the least recall value of the other two classification models. Overall, the SVM with HOG produced the most excellent precision value of the other two models, whereas the SVM with the Haralick feature extractor model had the lowest precision value.

Moreover, during the 50:50 training testing split ratio, the KNN, KNN with HOG feature extraction, and KNN with Haralick feature extractor models had the lowest accuracy of 83.32%, 82.68%, and 69.52%, respectively. Overall, the KNN with HOG feature extraction performed better and produced the highest accuracy value compared to the other two models. KNN with the Haralick feature extractor had the worst performance and obtained the lowest accuracy score among the three trained and tested models. The KNN model had the most outstanding recall value among the three models, whereas KNN with the Haralick feature extraction model had the least recall value of the other two classification models. Overall, the KNN with HOG produced the highest precision value of the other two models, whereas KNN with the Haralick feature extractor model had the lowest precision score.

As for Fork = 45, both KNN and KNN with Haralick feature extractor models achieved the highest accuracy

value of 87.56% and 75.55%, respectively, during the 90:10 training testing split ratio. Meanwhile, the KNN with HOG feature extraction had the maximum accuracy value of 85.91% during the 80:20 training testing split percentage. Moreover, during the 50:50 training testing split ratio, the KNN, KNN with HOG feature extraction, and KNN with Haralick feature extractor models had the lowest accuracy of 84.70%, 83.65%, and 72.20%, respectively. Overall, the KNN model performed better and produced the highest accuracy value compared to the other two models. KNN with the Haralick feature extractor had the worst performance and provided the lowest accuracy score among the three trained and tested models. The KNN model had the highest recall value among the three models, whereas KNN with the Haralick feature extraction model had the least recall value of the other two classification models. Overall, the KNN with HOG produced the most outstanding precision value of the other two models, whereas KNN with the Haralick feature extractor model had the lowest precision score.

With $k = 5$, the KNN model achieved the highest accuracy value of 87.69% during the 70:30 training testing split ratio; meanwhile, both KNN with HOG feature extraction and KNN with Haralick feature extractor had the maximum accuracy value of 86.32% and 79%, respectively, during 90:10 training testing split percentage. Moreover, during the 60:40 training split ratio, the KNN and KNN with Haralick feature extractor models had the lowest accuracy of 86.86% and 75.14%, respectively. KNN with the HOG feature extraction model obtained the highest accuracy score during the 50:50 training testing split ratio of 84.01%. Overall, the KNN model performed better and produced better accuracy than the other two.

The highest recall score obtained by the KNN model was during the 80:20 training testing split ratio with 92.22%, while the model achieved the lowest recall score of 90.58% during the 50:50 training testing split ratio. Next, the second model, KNN with HOG feature extraction, obtained the highest recall of 82.45% during the 80:20 training testing split percentage. The lowest recall score was during the 50:50 training testing split ratio of 79.45%. Then, the KNN with the Haralick feature extractor had the highest recall during the 90:10 training testing split percentage of 78.14%. It obtained a 73.59% recall value, the lowest during the 60:40 training testing split ratio. The KNN model had a better recall value among the three models, whereas KNN with the Haralick feature extraction model had the lowest recall value compared to the other two classification models. Overall, the KNN with HOG produced the highest precision value of the other two models, whereas KNN with the Haralick feature extractor model had the lowest precision score.

Table 3. Performance of SVM and its variants

Type of Kernels	Split Ratio	Accuracy (%)			Recall (%)			Precision (%)		
		SVM	SVM + HOG	SVM + HARALICK	SVM	SVM + HOG	SVM + HARALICK	SVM	SVM + HOG	SVM + HARALICK
Linear	50:50	79.97	86.39	71.51	81.04	86.81	63.21	78.26	86.43	76.56
	60:40	80.71	86.27	71.31	82.51	86.82	62.21	77.95	86.30	77.03
	70:30	82.11	87.14	72.58	84.13	87.03	64.00	79.17	87.31	78.09
	80:20	82.51	87.76	73.04	84.27	87.60	65.73	79.97	87.72	76.62
	90:10	83.56	88.12	74.17	85.21	86.61	68.30	81.21	89.54	77.88
Polynomial	50:50	89.07	91.92	49.36	90.48	93.62	2.00	87.33	90.75	1.00
	60:40	89.63	92.36	49.53	90.87	93.21	8.00	88.11	91.90	1.00
	70:30	90.27	93.31	50.50	91.61	94.37	27.00	88.66	92.61	1.00
	80:20	90.87	93.08	47.68	92.77	94.28	93.87	88.67	91.98	48.59
	90:10	91.02	92.67	50.00	91.59	93.44	90.43	90.33	92.18	50.30
RBF	50:50	89.65	89.62	67.80	92.78	91.11	60.54	86.00	88.74	71.63
	60:40	89.83	90.35	67.88	93.31	91.78	60.35	85.83	89.53	72.04
	70:30	91.05	90.64	69.03	94.23	91.38	61.65	87.37	92.61	73.19
	80:20	90.87	91.08	69.79	93.78	92.20	63.78	87.56	90.06	72.12
	90:10	91.43	90.60	68.50	94.37	92.07	62.29	88.12	89.62	71.69

Table 4. Performance of KNN and its variants

K-value	Split Ratio	Accuracy (%)			Recall (%)			Precision (%)		
		KNN	KNN + HOG	KNN + HARALICK	KNN	KNN + HOG	KNN + HARALICK	KNN	KNN + HOG	KNN + HARALICK
85	50:50	83.32	82.68	69.52	91.52	74.65	62.23	73.45	89.48	73.62
	60:40	83.71	83.23	70.48	92.36	75.42	64.76	73.53	90.03	74.03
	70:30	84.70	82.99	72.67	92.35	74.88	68.99	75.66	92.61	75.19
	80:20	85.27	85.14	72.90	92.51	78.55	69.77	76.79	90.24	74.11
	90:10	84.39	85.35	71.82	92.20	79.23	67.75	74.11	89.62	74.25
45	50:50	84.70	83.65	72.20	91.86	77.27	69.14	76.16	89.07	74.32
	60:40	84.89	84.79	72.45	92.58	78.34	68.77	75.58	90.50	75.03
	70:30	86.40	84.05	74.56	93.02	77.51	72.43	78.70	89.71	76.31
	80:20	86.93	86.10	74.15	93.21	80.22	73.39	79.69	90.70	74.22
	90:10	87.56	85.91	75.55	93.87	80.05	74.04	74.11	89.62	74.25
5	50:50	86.94	84.01	75.29	90.58	79.45	74.93	82.46	87.88	75.88
	60:40	86.86	85.58	75.14	91.26	81.46	73.59	81.54	89.28	76.66
	70:30	87.69	85.99	76.35	91.90	81.59	74.52	82.67	89.91	77.98
	80:20	87.49	86.24	77.19	92.22	82.45	75.90	81.90	89.02	77.63
	90:10	86.18	86.32	79.00	91.45	82.24	78.14	79.83	89.85	79.88

4. Conclusion

Two machine learning algorithms, SVM and KNN models have been used in the project for the classification process. Each algorithm also consists of three models: the basic model and HOG and Haralick feature extractions. All of these models can achieve and obtain good accuracy values. SVM with HOG feature extraction performed better and produced the highest accuracy, precision, and recall values than the other five models. It obtained an accuracy score of 93.31%, 94.37%, and 88.12%, respectively, for the recall and precision values.

Meanwhile, SVM with Haralick feature extraction produced the lowest accuracy value of 74.17%, a recall value of 68.30%, and a precision score of 77.88%. HOG has demonstrated a good performance in improving the SVM and KNN methods for image classification. In the future, HOG can be enhanced and tested with other machine learning and deep learning methods on balanced and imbalanced CXR images.

Funding Statement

This article was funded by Institute for Big Data Analytics and Artificial Intelligence (IBDAAI) and Universiti Teknologi MARA.

Acknowledgements

The authors would like to thank Institute for Big Data Analytics and Artificial Intelligence (IBDAAI), Universiti Teknologi MARA, Shah Alam, Malaysia, for providing essential support and knowledge to the authors.

References

- [1] H. Harapan, N. Itoh, A. Yufika, W. Winardi, S Keam, H. Te, H and M. Mudatsir, "Coronavirus Disease 2019 (Covid-19): A Literature Review," *Journal of Infection and Public Health*, vol. 13, no. 5, pp. 667-673, 2020.
- [2] T. Zhang, Q. Wu and Z. Zhang, "Probable Pangolin Origin of Sars-Cov-2 Associated with the Covid-19 Outbreak," *Current Biology*, vol. 30 no. 7, pp. 1346-1351, 2020.
- [3] S. R. Nayak, D. R. Nayak, U. Sinha, V. Arora and R. B. Pachori, "Application of Deep Learning Techniques for Detection of Covid-19 Cases Using Chest X-Ray Images: A Comprehensive Study," *Biomedical Signal Processing and Control*, vol. 64, pp. 102365, 2021.
- [4] C. Huang, Y. Wang, X. Li, L. Ren, J. Zhao, Y. Hu, L. Zhang, G. Fan, J. Xu, X. Gu, Z. Cheng, T. Yu, J. Xia, Y. Wei, W. Wu, X. Xie, W. Yin, H. Li, M. Liu. B. Cao, "Clinical Features of Patients Infected with 2019 Novel Coronavirus In Wuhan, China," *The Lancet*, vol. 395, no. 10223, pp. 497-506, 2020.
- [5] M. A. Khan, "An Automated and Fast System To Identify Covid-19 From X-Ray Radiograph of the Chest Using Image Processing and Machine Learning," *International Journal of Imaging Systems and Technology*, vol. 31, no. 2, pp. 499-508, 2021.
- [6] P. Kedia, Anjum, and R. Katarya, "Covent-19: A Deep Learning Model for the Detection and Analysis of Covid-19 Patients," *Applied Soft Computing*, vol. 104, 107184, 2021.
- [7] A. Kumar Das, S. Kalam, C. Kumar and D. Sinha, "TLC - An Automated Covid-19 Screening Model Using Transfer Learning from Chest X-Ray Images," *Chaos, Solitons & Fractals*, vol. 144, 110713, 2021.
- [8] S. Pathan, P. C. Siddalingaswamy and T. Ali, "Automated Detection of Covid-19 From Chest X-Ray Scans Using an Optimized CNN Architecture," *Applied Soft Computing*, vol. 104, 107238, 2021.
- [9] G. Pascarella, A. Strumia, C. Piliago, F. Bruno, R. Del Buono, F. Costa, S. Scarlata and F. E. Agrò., "Covid-19 Diagnosis and Management: A Comprehensive Review," *Journal of Internal Medicine*, vol. 288, no. 2, pp. 192-206, 2020.
- [10] Tian Jipeng, Manasa S., Dr. T.C.Manjunath, "Early Detection of Eye Disease in Humans Using Random Forest & Hog Concepts," *SSRG International Journal of Electronics and Communication Engineering*, vol. 7, no. 4, pp. 5-7, 2020. Crossref, <https://doi.org/10.14445/23488549/IJECE-V7I4P102>.
- [11] Z. Gao, Y. Xu, C. Sun, X. Wang, Y. Guo, S. Qiu, and K. Ma, "A Systematic Review of Asymptomatic Infections with Covid-19," *Journal of Microbiology, Immunology and Infection*, vol. 54, no. 1, pp. 12-16, 2020.
- [12] A. Abbas, M. Abdelsamea, and M. M. Gaber, "Classification of Covid-19 in Chest X-Ray Images Using Detrac Deep Convolutional Neural Network," *2020 IEEE 6th International Conference on Computer and Communications, ICC3 2020*, pp. 426-433, 2020.
- [13] F. I. M. Redzuan and M. Yusoff, "Knots Timber Detection and Classification with C-Support Vector Machine," *Bulletin of Electrical Engineering and Informatics*, vol. 8, no. 1, pp. 246-252, 2019.
- [14] V. N. M. Aradhya, M. Mahmud, D. S. Guru, B. Agarwal, and M. S. Kaiser, "One-Shot Cluster-Based Approach for the Detection of Covid-19 From Chest X-Ray Images," *Cognitive Computation*, vol.13, no. 4, pp. 873-881, 2021.
- [15] A. Suleiman, Y. H. Chen, J. Emer and V. Sze, "Towards Closing the Energy Gap Between Hog and Cnn Features for Embedded Vision," In *2017 IEEE International Symposium on Circuits and Systems (ISCAS)*, pp. 1-4, 2017.
- [16] A. M. Ayalew, A. O. Salau, B. T. Abeje and B. Enyew, "Detection and Classification of Covid-19 Disease From X-Ray Images Using Convolutional Neural Networks and Histogram of Oriented Gradients," *Biomedical Signal Processing and Control*, pp. 103530, 2022.
- [17] M. Jawahar, J. Prassanna, V. Ravi, L. J. Anbarasi, S. G. Jasmine, R. Manikandan ... and S. Kannan, "Computer-Aided Diagnosis of Covid-19 From Chest X-Ray Images Using Histogram-Oriented Gradient Features and Random Forest Classifier," *Multimedia Tools and Applications*, pp. 1-18, 2022.
- [18] T. Löfstedt, P. Brynolfsson, T. Asklund, T. Nyholm and A. Garpebring, "Gray-Level Invariant Haralick Texture Features," *Plos One*, vol. 14, no. 2, pp. E0212110, 2019.
- [19] E. Miyamoto, and T. Merryman, "Fast Calculation of Haralick Texture Features," *Human-Computer Interaction Institute, Carnegie Mellon University, Pittsburgh, Usa. Japanese Restaurant Office*, 2005.
- [20] B. Dhruv, N. Mittal, and M. Modi, M, "Study of Haralick's and Glcm Texture Analysis on 3d Medical Images," *International Journal of Neuroscience*, vol. 129, no. 4, pp. 350-362, 2019.
- [21] Simonthomas, N. Thulasi and P. Asharaf, "Automated Diagnosis of Glaucoma Using Haralick Texture Features," In *International Conference on Information Communication and Embedded Systems (ICICES2014)*, IEEE, pp. 1-6, 2014.

- [22] J. Weibel, J. Gola, D. Britz and F. Mücklich, "A New Analysis Approach Based on Haralick Texture Features for the Characterization of Microstructure on the Example of Low-Alloy Steels," *Materials Characterization*, vol. 144, pp. 584-596, 2018.
- [23] M. A. Khan, "An Automated and Fast System To Identify Covid-19 From X-Ray Radiograph of the Chest Using Image Processing and Machine Learning," *International Journal of Imaging Systems and Technology*, vol. 31, no. 2, pp. 499-508, 2021.
- [24] Abbas, M. M. Abdelsamea, and M. M. Gaber, "Classification of Covid-19 In Chest X-Ray Images Using Detrac Deep Convolutional Neural Network," *Applied Intelligence*, vol. 51, no. 2, pp. 854-864, 2021.
- [25] I. Arpacı, I. S. Huang, M. Al-Emran, M. N. Al-Kabi and M. Peng, "Predicting the Covid-19 Infection with Fourteen Clinical Features Using Machine Learning Classification Algorithms," *Multimedia Tools and Applications*, vol. 80, no. 8, pp. 11943-11957, 2021,
- [26] L. J. Muhammad, E. A. Algehyne, S. S. Usman, A. Ahmad, C. Chakraborty and I. A. Mohammed, "Supervised Machine Learning Models for Prediction of Covid-19 Infection Using Epidemiology Dataset," *SN Computer Science*, vol. 2, no. 1, pp. 1-13, 2021.
- [27] E. Al Mamlook, S. Chen and H. F. Bzizi, "Investigation of the Performance of Machine Learning Classifiers for Pneumonia Detection In Chest X-Ray Images," *IEEE International Conference on Electro Information Technology*, pp. 98-10, 2022.
- [28] Yarui Wang, Zuolei Sun, Xiaoyu Wang "Adaptive Target Tracking Based on Kernel Svm and Hog Features," *International Journal of Recent Engineering Science*, vol. 5, no. 1, pp. 11-15, 2018. Crossref, <https://doi.org/10.14445/23497157/IJRES-V5I1P103>.
- [29] Kaggle. (Accessed on 10 March 2022). Available Online: https://www.kaggle.com/Tawsifurrahman/Covid19-Radiography-Database?fbclid=Iwar0rw_Prtvf9r0zinrjqtfaezebaesxh3rb60tdrpdawjdonebil2nf6epk.
- [30] Q. Wu and D. X. Zhou, "Analysis of Support Vector Machine Classification," *Journal of Computational Analysis and Applications*, vol. 8, no. 2, pp. 99-119, 2006.
- [31] D. K. Srivastava and L. Bhambh, "Data Classification Using Support Vector Machine," *Proceedings - International Conference on Tools with Artificial Intelligence, ICTAI*, vol. 1, pp. 3-6, 2010.
- [32] J. Kim, B. -S. Kim and S. Savarese, "Comparing Image Classification Methods: K-Nearest-Neighbor and Support-Vector-Machines," *Applied Mathematics in Electrical and Computer Engineering*, pp. 133-138, 2012.
- [33] M. K. S. Varma, N. K. K. Rao, K. K. Raju and G. P. S. Varma, "Pixel-Based Classification Using Support Vector Machine Classifier," *Proceedings - 6th International Advanced Computing Conference, IACC*, 2016.
- [34] Q. Z. Song, L. Zhao, X. K. Luo and X. C. Dou, "Using Deep Learning for Classification of Lung Nodules on Computed Tomography Images," *Journal of Healthcare Engineering*, 2017.
- [35] V. Sharma, A. Kumar, L. Panat, G. Karajkhede and A. Lele, "A Malaria Outbreak Prediction Model Using Machine Learning," *International Journal of Advanced Research in Computer Engineering & Technology*, vol. 4, no. 12, pp. 4415-4419, 2015.